

# Formation of stars from dark matter clumps of primordial planets

Carl H. Gibson<sup>1,3</sup>, Rudolph E. Schild<sup>2</sup>, N. Chandra Wickramasinghe<sup>3</sup> and Theo M. Nieuwenhuizen<sup>4</sup>

<sup>1</sup> Mech. and Aerospace. Eng. & Scripps Inst. of Oceanography Depts., UCSD, La Jolla, CA 92093-0411, USA

<sup>2</sup> Harvard-Smithsonian Center for Astrophysics, 60 Garden Street, Cambridge, MA02138, USA

<sup>3</sup> Buckingham Centre for Astrobiology, The University of Buckingham, Buckingham MK18 1EG, UK

<sup>4</sup>Institute for Theoretical Physics, Science Park 904, P.O. Box 94485, Amsterdam, the Netherlands

E-mail: cgibson@ucsd.edu

**Abstract.** Observations of the interstellar medium by the Herschel, Planck etc. infrared satellites throw doubt on  $\Lambda$ CDMHC cosmology and its associated mechanisms of star formation from gas and dust. According to the Hydro-Gravitational-Dynamics (HGD) cosmology of Gibson (1996), and the observations of Schild (1996), the dark matter of galaxies consists of Proto-Globular-star-Cluster (PGC) clumps of Earth-mass primordial gas planets in metastable equilibrium since Planet mergers within PGCs began star production at 0.3 Myr. Within a Gyr, clumps of PGCs began diffusion from the Milky Way protoGalaxy, upon freezing at 14 Myr, to give the Magellanic Clouds and the faint dwarf galaxies of the  $10^{22}$  m diameter baryonic dark matter Galaxy halo. The first stars persist as old globular star clusters (OGCs). Old stars more massive than  $1.44M_{\odot}$  never existed in this model, and may never exist with any age. Mysterious (by  $\Lambda$ CDMHC) damped Lyman- $\alpha$  (DLA) galaxies show sizes and metallicities easily explained by HGD.

## 1. Introduction

The standard cosmological model  $\Lambda$ CDMHC is thrown into doubt by recent observations by infrared satellites (Gibson, Schild & Wickramasinghe 2011). We have argued that the dark ages of the standard model without stars or planets for  $\geq 300$  Myr would have prevented formation of life and its cosmic distribution. In our model dark energy and a cosmological constant  $\Lambda$  are also unnecessary; Cold-Dark-Matter (CDM) is also unnecessary and never existed. Clumps of CDM collisionless particles do not (and cannot) exist, and cannot Hierarchically Cluster (HC) to form non-baryonic dark matter halos of galaxies. The standard cosmological model fails because it makes incorrect assumptions about the fluid mechanics of gravitational structure formation. Viscous forces are neglected and turbulence is ignored, and fossil turbulence and fossil turbulence waves are not mentioned. Molecular diffusion is not taken into account.

An alternative cosmology is provided by the fluid mechanical theory of Gibson (1996), termed Hydro-Gravitational-Dynamics (HGD) cosmology, and the independent quasar microlensing observations and physical interpretation of Schild (1996) leads to the same conclusion; that is, that the dark matter of galaxies is planets. Most of the power radiated by the CMB is supplied by planet mergers. According to HGD theory and the Schild observations,  $3 \times 10^7$  Earth-mass primordial gas planets exist per star in Proto-Globular-star-Cluster (PGC) clumps in all galaxies. This is thirty times the mass of the stars. In this paper we focus on the formation of stars from planets as supported by data from Herschel, Planck and other infrared telescopes. Powerful infrared radiation is emitted by planet mergers within PGCs as larger planets and stars form in HGD cosmology. The dominant form of galaxy dark matter is dark in the visible but not dark in the infrared.

HGD cosmology predicts photon-viscosity fragmentation of the expanding plasma universe at time  $10^{12}$  seconds (30,000 years), as shown in Table 1. Fragmentation is at supercluster mass ( $10^{47}$  kg) and Hubble length ( $L_H = ct = 3 \times 10^{20}$  m) scales, and produced weak turbulence and fossil turbulence density and vorticity at the stratified void boundaries.

The baryonic density of the fragments matches that of old globular star cluster OGCs ( $\rho_0 = 4 \times 10^{-17}$  kg m<sup>-3</sup>). Proof of this event is that supervoids are observed to be at least ten times larger than superclusters ( $10^{25}$  m versus  $10^{24}$  m).

| Event                         | Time (seconds)           |
|-------------------------------|--------------------------|
| Big Bang                      | $10^{-43}$ to $10^{-27}$ |
| Nucleosynthesis               | $10^2$                   |
| Matter exceeds Energy         | $10^{11}$                |
| Plasma supercluster fragments | $10^{12}$                |
| Plasma galaxy fragments       | $10^{13}$                |
| Gas galaxy fragments          | $10^{13} + 10^{12}$      |
| First stars and supernovae    | $10^{13} + 10^{12}$      |
| First water oceans and life   | $10^{14}$                |

Table 1: Timeline of HGD cosmology.

According to  $\Lambda$ CDMHC cosmology, gravitational structure forms within CDM halos, starts at small scales, and hierarchically clusters (HC) to supercluster scales. The supercluster voids should be the last structures to form, and should be smaller than the superclusters themselves, which have scale  $10^{24}$  meters.

It is easy to understand how supervoids can become ten times larger than superclusters from HGD since both begin at the same time ( $10^{12}$  seconds in Table 1), and the growth of voids is enhanced by the expansion of the universe while the growth of superclusters is inhibited. Origin of void-cluster separation on Gpc scales is demonstrated in the Hutsmeckers et al. (2011) observation of cosmological cells with aligned polarization structure. These imply a rotational formation originating in a turbulence and fossil turbulence process, and possibly a remnant rotation of the universe.

The scale of fragmentation decreases to that of proto-galaxies in the plasma until photons decouple from collisions with electrons at the plasma-to-gas transition ( $10^{13}$  seconds in Table 1). A turbulent and fossil turbulent origin of the internal rotation of galaxies in Abell 1689 is implied by the observation that the galaxy spins within the cluster are aligned (Hung, L. et al., 2010).

The gas promptly fragments at two mass scales: the mass of PGCs and the mass of small planets, for (fluid mechanical) reasons discussed in Section 2. The time required for the proto-galaxies to fragment is the gravitational free fall time of the gas, which is preserved as a fossil of the initial (viscous-gravitational) fragmentation time of the plasma along with the density and rate of strain. Hence, the first stars and supernovae occur promptly, transporting the first chemicals such as carbon, oxygen, nitrogen, silicon and iron to the primordial planets.

The strongly reducing hydrogen atmospheres of the planets convert the iron and nickel oxides from supernovae to condensing droplets of these liquid metals that sink to the planet centers, followed by condensing rains of vaporized rocks. The plasma-gas transition temperature ( $T \approx 3000$  K) matches the boiling point of stainless steel. Finally, hot water oceans condense at about two million years when the planets cool to the 647 K critical temperature of water. Complex organic chemical reactions leading to

life formation are most likely to have formed in the warm oceans of the planets between two million years and eight million years, after which the oceans will begin to freeze. This is the biological big bang and represents the inception of life in the cosmos (Gibson, Wickramasinghe and Schild (2011), Wickramasinghe (2010)).

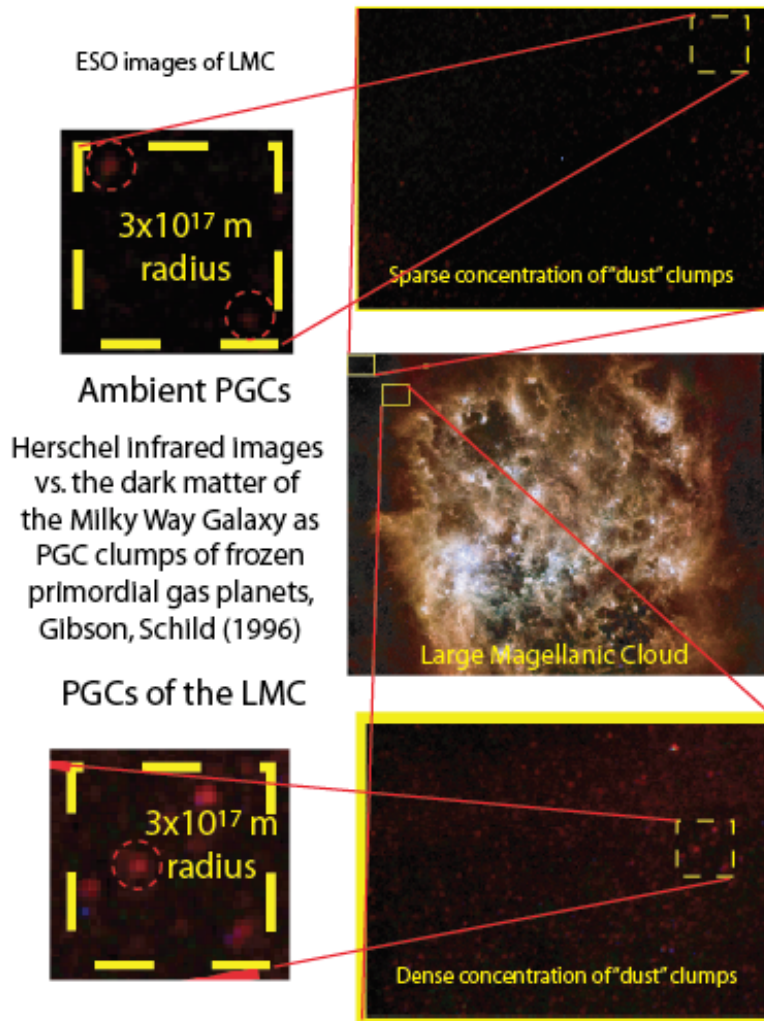


**Figure 1.** Large Magellanic Cloud (right center) infrared images versus the predictions of HGD cosmology. Red dot dust clumps (dashed circles) are clearly the galaxy dark matter PGC clumps of frozen primordial gas planets claimed by Gibson, Schild (1996). Underlying ESO, NASA, JPL images.

Figure 1 on page 4 shows Herschel infrared frequency high resolution images of dark matter PGC clumps of planets, concealed as red dot PGCs in the Large Magellanic Cloud dwarf galaxy of the Southern Hemisphere. The baryonic dark matter is not at all dark at these sub-mm (0.2mm) frequencies. The PGCs glow with highly variable brightness but the same size, matching the  $3 \times 10^{17}$  m radius predicted by HGD theory as shown by the highest resolution images on the left. Gravitational potential energy of the planets is released as they merge to form larger planets. When sufficiently large numbers of large frozen hydrogen planets are formed in binary mergers, an Oort cavity cold core

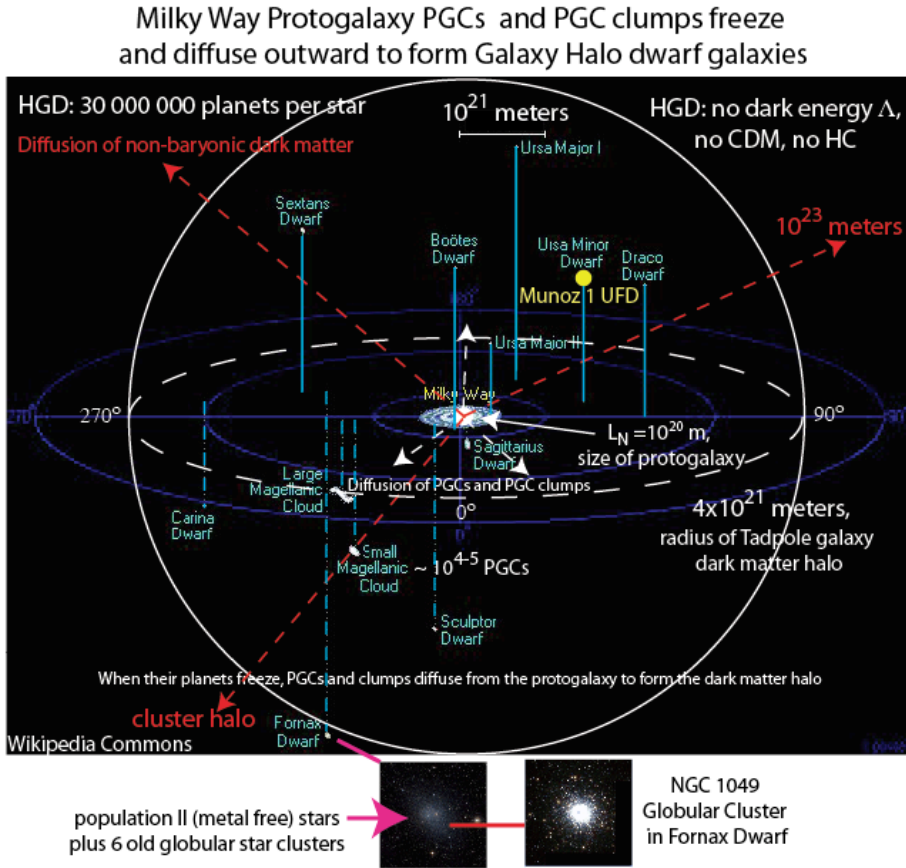


**Figure 2.** Distribution of dark matter in Milky Way galaxy according to HGD cosmology. The non-baryonic dark matter has diffused to form galaxy cluster and supercluster halos at Schwarz diffusive scales  $L_{SD} \approx 10^{23}$  m (red dashed arrows). When the central proto-galaxy at Nomura scale  $L_N = 10^{20}$  m and density  $\rho_0$  cooled to the hydrogen triple point temperature 13.8 K, frozen PGCs and clumps of PGCs began diffusing away from the core (dashed white arrows) to form the Galaxy dark matter halo, with diameter  $\approx 10^{22}$  m. Underlying images from Wikipedia.

$((M_{\odot}/\rho_0)^{1/3})$  is formed in the PGC at the triple point temperature of hydrogen 13.8 K.

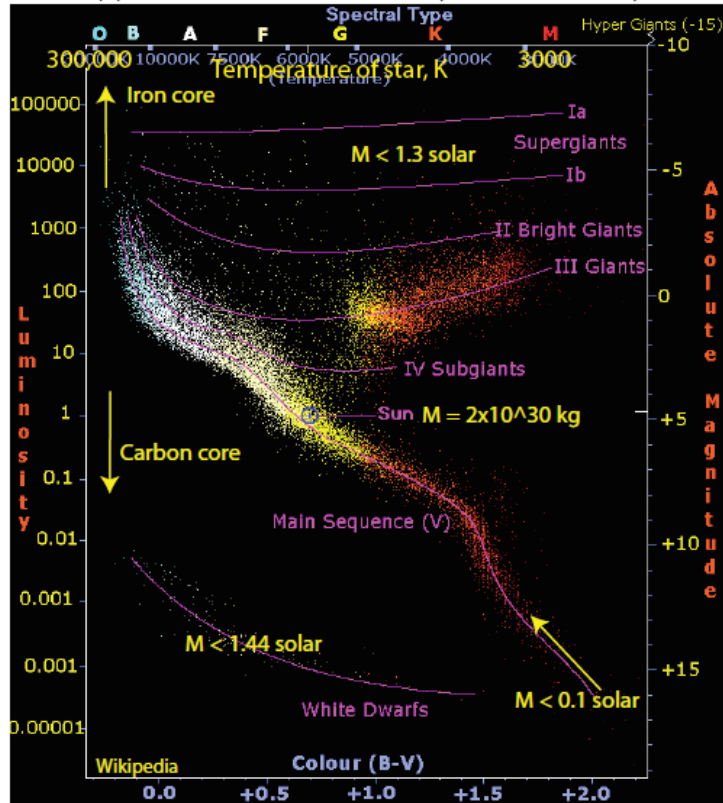
Red lines show the locations and sizes of the dashed line yellow boxes where the very high resolution images are located. The ambient density of PGCs is shown by the two images at the top of Fig. 1, and the large LMC density of PGCs is shown by the two images at the bottom. The red dots are unlikely in our view to be ceramic dust in cirrus clouds as claimed by the standard model.

In the following we focus on star formation theory. As we see from Fig. 1, stars are not formed from gas and dust in CDM halos. They are formed in PGCs from merging planets. Consequently, many aspects of star formation such as the Hertzsprung-Russell diagram must be revisited since the present picture does not include post-formation absorption of the primordial planets. In the HGD picture, primordial planets were hot and extended in the early universe. Moreover the universe was much denser at the

Hertzsprung-Russell diagram must be modified to take primordial dark matter planets into account:

1. star masses are overestimated
2. star lifetimes are underestimated

O,B,A star masses less than 1.3 solar (not 15 to > 50 solar)



From HGD cosmology, there are no massive stars with  $M > 1.44$  Solar

**Figure 3.** Hertzsprung-Russell luminosity-temperature diagram for HGD star formation. Stars appear to be massive when they are bright from a rapid rate of dark matter planet accretion (eg: O and B stars do NOT have mass  $\geq 1.3$  solar, a neutron star mass). The iron core stars that produce supernovae II and neutron stars are less massive than the carbon core stars that produce supernovae I events. Underlying image from Wikipedia.

earliest epochs of star formation. Both these factors would have increased likelihood of rapid planet ingestion by an early generation stars in all phases of evolution. A gradually slowing, continued infall of primordial planets is likely to have happened until the universe had cooled to below the hydrogen condensation temperature at approximately 14 Myr, shrinking the primordial planets extended hydrogen atmospheres.

The existence of dark matter planets is bolstered by the continuous discovery of unexpected exoplanets at rates accelerated by new infrared satellites such as WISE (Wright et al. 2010). Present discoveries of exoplanets surrounding stars in the solar neighborhood have demonstrated the existence of surprising numbers of super-jupiters in close orbits that would put them within red giant atmospheres, possibly explaining blue stragglers. The well-known mysterious “third parameter” needed to describe color-

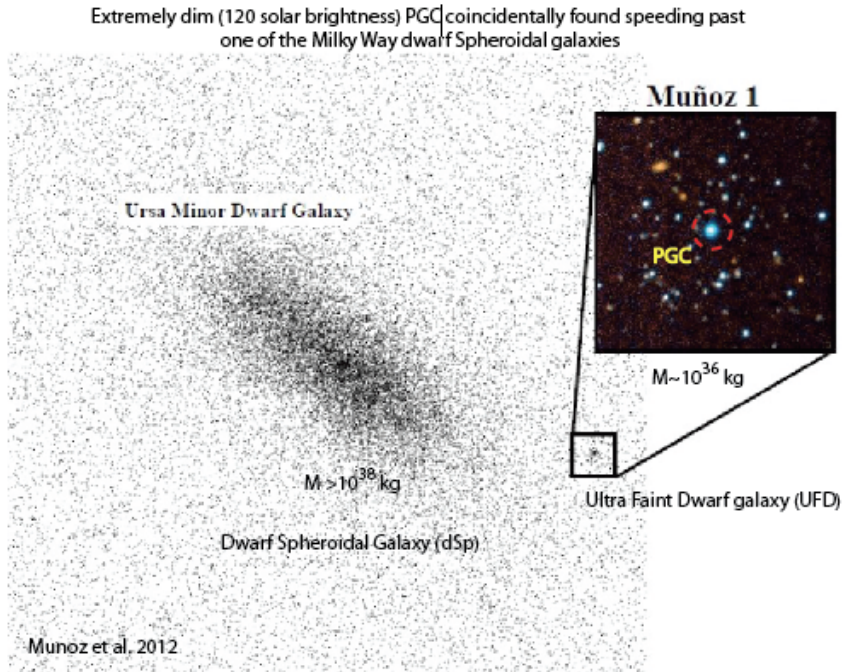


**Figure 4.** A very faint ( $\approx 500$  star) old globular star cluster (OGC) detected (coincidentally) in the Ursa Minor Dwarf Galaxy. According to HGD cosmology, Munoz 1 is one of the many ( $\approx 1000$  ultra-faint-dwarf (UFD) galaxies found in the Milky Way Halo as dark matter. Such UFDs and the LMC and SMC galaxies (each with  $\approx 10^4$  PGCs) originated when the PGCs of the Milky Way protogalaxy (PG) became cold (13.8 K) enough for their planets to freeze, about 14 million years after the big bang. At this time the PGCs became weakly collisional and began to diffuse away from the central  $10^{20}$  m (Nomura scale) PG to form the present  $10^{22}$  m diameter Galaxy halo. The distance to Munoz 1 is  $1.5 \times 10^{21}$  m (Munoz et al. 2012), so it is well within the MW halo. Only 100-500 stars have formed in Munoz 1, from the  $10^6 M_{\odot}$  possible, giving a dark/luminous mass ratio of  $\geq 2000$ . Image from Munoz et al. 2012.

magnitude diagram differences of ancient globular clusters with known comparable ages and chemistries (Richer et al., 1996) might well represent a rate of mass ingestion.

Figure 2 on page 5 shows the HGD interpretation of the Milky Way Galaxy. Brown et al. (2012) discuss a class of ultra-faint-dwarf galaxies (UFDs) recently detected by the Hubble Space Telescope. These dark matter dominated objects are easily explained by HGD as diffusion of PGCs and clumps of PGCs away from the protoGalaxy on freezing of the planets at 14 Myr.

Figure 3 on page 6 shows the HGD interpretation of the Hertzsprung-Russell diagram. When stars form from merging planets rather than from gas and dust, it is no longer necessary to assume that the stars are more massive than the instability limit of supernovae precursors.

Figure 4 on page 7 shows the HGD interpretation of a recently detected (UFD) dim globular cluster (Munoz 1), coincidentally passing in front of one of the Milky Ways dwarf spheroidal galaxies (Ursa Minor), Munoz et al. (2012).

Figure 5 on page 10 shows the HGD interpretation of recently detected Damped Lyman- $\alpha$  galaxies classified by size and metallicity, Krogager et al. (2012).

## 2. Theory

As shown in Table 1, the initial big bang and inflation events of the universe occurred in a short time interval at small scales and high temperatures, and can be easily understood using basic fluid mechanical concepts of turbulence, fossil turbulence and kinematic viscosity (Gibson 2004, 2005). Turbulence cascades from small scales to large, limited by inertial-vortex forces. Kolmogorovian universal similarity applies. The relevant dimensional parameters are  $c, h, G$  and  $k$ , where  $c$  is light speed and  $h, G, k$  are the universal constants of Planck, Newton and Boltzmann. Turbulence occurs because only Planck particles can exist at Planck temperatures, so the collision distance is the Planck length scale, which matches the Kolmogorov scale.

The HGD big bang turbulence mechanism is where a Planck particle and a Planck anti-particle combine to form a spinning particle similar to electron-positron positronium particles in supernovae. At Planck temperatures from the Kerr metric a prograde accretion of a Planck particle yields 42% of the rest mass energy, Peacock (2000), producing a spinning gas of more Planck particles. Details and references may be found in Volume 18 of the *Journal of Cosmology*. This was the first turbulent combustion event. Fossils of big bang turbulence are preserved in all aspects of astrophysics, astronomy and cosmology, particularly those that involve spin. Symmetry between matter and antimatter was achieved by the prograde accretion of an anti-Planck particle by a Planck pair. This set the direction of the spin and the fate of the universe not to be antimatter. The big bang was a unique time of absolute instability for nonlinear turbulence and nonlinear gravity. Reynolds numbers of a million were possible at first because the collision distance was the Planck scale  $L_P = 10^{-35}$  m. Little entropy was produced by the turbulence because the temperature  $T_P = 10^{32}$  K was so large.

Viscosity became important when the big bang cooled enough to permit quarks and gluons to exist. Gluons transmit momentum over scales much larger than the Planck scale  $10^{-35}$  m. Gluon viscous stresses were negative, extracting sufficient mass-energy from the vacuum, according to Einstein's general relativity equations, for the present universe with its  $10^{80}$  primordial gas planets. Turbulence was prevented by viscous stresses because the Schwarz viscous-gravitation scale  $L_{SV} = [(\gamma\nu)/(\rho G)]^{1/2}$  was so much larger than the scale of causal connection  $L_H = ct$ , where  $\gamma = 1/t$  is the rate-of-strain,  $\nu$  is the kinematic viscosity,  $\rho$  is the density,  $t$  is time,  $c$  is light speed, and  $G$  is Newton's gravitational constant.

Fragmentation occurred at  $t = 10^{12}$  s when  $L_H = L_{SV}$ . The viscosity of the plasma was determined by photon-electron elastic collisions, with  $\nu = 4 \times 10^{26}$  m<sup>2</sup> s<sup>-1</sup>. The fragmentation mass was that of superclusters,  $\approx 10^{47}$  kg. Despite the large viscosity, baroclinic torques of the fragmentation could produce weak turbulence in the plasma and determine the morphology of the protoclusters and protogalaxies formed as the

fragmentation mass decreased to that of galaxies  $\approx 10^{44}$  kg.

The kinematic viscosity of the primordial gas at plasma-gas transition decreased by a factor of a trillion to  $\nu \approx 10^{13} \text{ m}^2 \text{ s}^{-1}$ , with corresponding decrease in the fragmentation mass in the protogalaxies to small planet values  $\approx 10^{25}$  kg. Because heat transfer in the gas was by radiation at the speed of light, and because pressure transfer was at sound speeds, an additional fragmentation occurred at the Jeans scale  $L_J = (V_S)/(\rho G)^{1/2}$ , where  $V_S$  is the speed of sound. The Jeans mass was  $10^6 M_\odot$ . Thus, galaxies emerged from the plasma epoch as 100% dark matter.

The non-baryonic component of protogalaxies is unknown except for the neutrinos. It has higher diffusivity than the baryons by a factor of about  $10^{20}$  and is more massive by a factor of about thirty. The fragmentation length is therefore significantly larger, comparable to the Schwarz diffusive gravitational scale  $L_{SD} = (D^2/\rho G)^{1/4}$ , where  $D$  is the diffusivity. The present non-baryonic dark matter halo size is about  $10^{23}$  m, as shown by the red dashed arrows in Fig. 2.

### 3. Observations

A flood of new observations at infrared frequencies shows stars and larger planets forming from the dark matter planets within PGCs. An example is shown in Figure 1 (right central image), from Herschel, of the Large Magellanic cloud. High resolution details of the image are captured in the yellow boxes in the upper left hand corner, and expanded to show details at the top and bottom right. These are expanded to show even finer detail in the top and bottom images on the left. What are the "red dot" objects that appear in the (dashed yellow box) highest resolution images? What we see is that the origin of the stars is thousands of PGCs, which can now be counted since they glow in the infrared.

Counts of PGCs from the ESO Herschel images are in progress. Preliminary estimates from the SMC are  $10^4$  to  $10^5$ , suggesting these dark matter objects have mass  $10^{10} \times M_\odot$  to  $10^{11} \times M_\odot$ , consistent with the usual assumptions of the mass of these galaxies.

### 4. Discussion

Star formation has been shown to be from planet mergers, not from condensation of gas and dust. Recent observations of DLA (damped Lyman- $\alpha$ ) galaxy sizes and metallicities are reported by Krogager et al. (2012), Figure 5 on page 10. Wolfe et al. (1986, 2003ab) pioneered the study of these early galaxies selected by their capability of detecting star forming regions. Surprisingly, the size of large red shift DLA galaxies was significantly larger than present DLA galaxies, as shown in the figure (green dashed line compared to blue dashed line). By the standard model, galaxies form by hierarchical clustering, so the redshift  $z \geq 2$  DLA galaxies should be smaller, not larger.

The ten new DLA galaxies presented show a remarkable, but unexplained, set of

correlations between size and metallicity. It is very clear from HGD cosmology why the dimmest and smallest DLA galaxies have such small metallicities. These are the dimmest of the infrared galaxies, with luminosity seven decades smaller than the brightest. They have the same mass as all other galaxies, but it is almost entirely frozen primordial planets in PGC clumps, which never actively formed stars and therefore have had only minimal metal enhancement of their primordial compositions. These are potentially the next generation of LIRGs (Luminous Infrared Galaxies). We predict that from HGD theory the abundances of their young stars will be close to the primordial values, with low metal abundances.

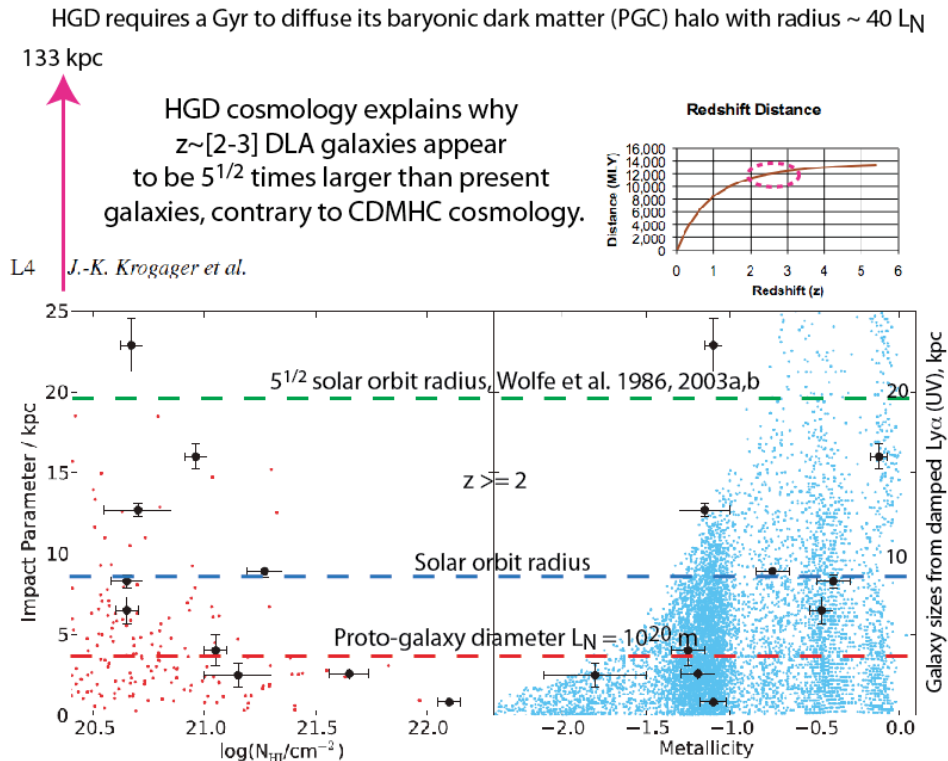


Figure 3. Impact parameters plotted against H I column density (left) and metallicity (right) for  $z \gtrsim 2$  DLA galaxies with securely identified galaxy counterparts (see Table 1). The observed impact parameters have been converted to kpc at redshift  $z = 3$  instead of arcsec for easier comparison. The blue points in the right-hand panel show the simulated distribution of impact parameters as a function of metallicity for DLA galaxies at  $z = 3$  from the model in Fynbo et al. (2008). The red points in the left-hand panel show model points from Pontzen et al. (2008).

**Figure 5.** Damped Lyman Alpha (DLA) observations of Wolfe et al. 1986, 2003a,b suggested something must be wrong with the standard CDMHC cosmology that predicts small initial galaxy size. From star formation rates implied by large DLA impact parameters (sizes) the early galaxies appeared to be larger than at present by about a factor of  $5^{1/2}$ . The impact parameter (galaxy size) versus ionized hydrogen and metallicity correlations of Krogager et al. 2012 are easy to understand from HGD cosmology, but are inexplicable from CDMHC cosmology (which should be abandoned). The very small size galaxies (center) have low metallicity both in the central  $L_N$  scale central region and in the metal free PGC dark matter halo, which diffuses to distances of over a hundred kpc in less than a billion years after the PGC planets freeze at 14 Myr. Underlying image and caption from Krogager et al. 2012, their Fig. 3.

## 5. Summary and Conclusions

Evidence from infrared telescopes makes the standard model of star formation seem untenable. Tens of thousands of PGC clumps of Earth-mass gas planets are now visible in the Milky Way galaxy, glowing brightly from mergers of the trillion planets per protoglobular-star-cluster as they make larger planets and eventually stars. The size of the observed PGCs matches the Gibson (1996) HGD predicted radius of  $3 \times 10^{17}$  m, which is a constant of the universe from HGD cosmology. The numbers of PGCs detected and inferred in the Milky Way galaxy and its halo match the Schild (1996) observational conclusion that vast numbers of rogue planets comprise the missing mass of galaxies,  $\approx 10^{17}$  planets per galaxy since  $10^{13}$  seconds (0.3 Myr) after the big bang from the HGD timeline of Table 1. So many hot hydrogen gas planets forming so soon after the first stars and supernovae were ideal hosts for life in the first oceans of the biological big bang, vindicating the Hoyle-Wickramasinghe hypothesis that life exists throughout most of cosmic space-time.

## 6. References

- [1] Brown, T.M., Tumlinson, J., Geha, M. et al., 2012, ApJL (accepted), arXiv:1206.0941v1 [astro-ph.CO]
- [2] Colley, W. et al, 2002, ApJ, 565, 105
- [3] Colley, W. et al, 2003, ApJ, 587, 71
- [4] Colley, W. & Schild, R. 2003, ApJ, 594, 97
- [5] Gibson, C. H. 1996 Appl. Mech. Rev. **49**, 299–315
- [6] Gibson, C. H. 2011 Journal of Cosmology **15**, 6030–6053
- [7] Gibson, C. H. 2012 Physica Scripta Proceedings, Turbulent Mixing and Beyond 2011 Trieste.
- [8] Gibson, C. H., Schild, R. E. and Wickramasinghe, N. C. 2011, Int. J. of Astrobiology 10 (2) : 83–98, doi:10.1017/S1473550410000352
- [9] Gibson, C. H., Wickramasinghe, N. C. and Schild, R. E. 2011, J. of Cosmology, 16, 6500-6518
- [10] Hung, L. et al., 2010, ApJ, 720, 1483
- [11] Hutsemekers, D. et al., 2011, ASPC, 449, 441
- [12] Krogager, J. K, J. P. U. Fynbo, P. Miller, C. Ledoux, P. Noterdaeme, L. Christensen, B. Milvang-Jensen and M. Sparre 2012, Mon. Not. Roy. Ast. Soc. Lett. accepted April 10, doi:10.1111/j.1745-3933.2012.01272.x
- [13] Munoz, R. R., Geha, M., Cote, P. et al. 2012, ApJ L (submitted)
- [14] Nieuwenhuizen, T. M. *Explanation of the Helium-3 problem*, J. Cos. 15, 6200 (2011).
- [15] Nieuwenhuizen, T. M., Gibson, C. H. & Schild, R. E. 2009 Europhys. Lett. **88**, 49001,1–6
- [16] Nieuwenhuizen, Th. M., Schild, R. E., Gibson, C. H., 2010, arXiv:1011.2530 J. Cosm.
- [17] Peacock, J.A., 2000, Cosmological Physics, Cambridge Univ. Press
- [18] Richer, H. B., et al. 1996, ApJ, 463, 602
- [19] Schild, R. E. 1996 Astroph. J. **464**, 125–130
- [20] Schild, R. E. 1999 Astroph. J. **514**, 598–606
- [21] Schild, R. E. 2005, AJ, 129, 1225
- [22] Schild, R. Leiter, D. & Robertson, S. 2006, AJ, 132, 420 (SLR06)
- [23] Schild, R. E. & Vakulik, V. 2003 AJ **126**, 689–695
- [24] Sumi, T. et al 2010 Astroph. J. **710**. 1641–1653

- [25] Sumi, T. et al. *Nature*, Volume 473, Issue 7347, pp. 349-352 (2011).
- [26] Wickramasinghe, N.C., 2010, *Int. J. Astrobiol.*, 9(2), 119-129, 2010, doi: 10.1017/S14735504099990413.
- [27] Wolfe A. M., Turnshek D. A., Smith H. E., Cohen R. D., 1986, *ApJS*, 61, 249
- [28] Wolfe, A. M., Gawiser, E., & Prochaska, J. X. 2003a, *ApJ*, 593, 215
- [29] Wolfe, A. M., Gawiser, E., & Prochaska, J. X. 2003b, *ApJ*, 593, 235
- [30] Wright, E. L., et al. 2010, *AJ*, 140, 1868